EUROPEAN JOURNAL OF PURE AND APPLIED MATHEMATICS
2025, Vol. 18, Issue 3, Article Number 6248
ISSN 1307-5543 – ejpam.com
Published by New York Business Global

Self-Similar Solutions to the Lin–Reissner–Tsien Equation via the Power Index Method

Zeshan Haider[1,*], Khalil Ahmad[1], Muhammad Shoaib Arif[2], Ateeq Ur Rehman[2], Muhammad Noman Qureshi[1]

[1] *Department of Mathematics, Faculty of Basic and Applied Sciences, Air University, PAF Complex E-9, Islamabad 44000, Pakistan*
[2] *Department of Mathematics and Sciences, College of Humanities and Sciences, Prince Sultan University, Riyadh 11586, Saudi Arabia*

Abstract. In this paper, the $(2+1)$-dimensional Lin–Reissner–Tsien (LRT) equation is investigated using the Power Index Method (PIM). A self-similar transformation is applied to reduce the given partial differential equation (PDE) into an ordinary differential equation (ODE) through a change of variables based on scaling symmetry. The analytic solution of the resulting ODE is obtained using the symbolic computation software Maple 18 and basic techniques. The self-similar solutions of the LRT equation are then derived by combining the ODE solution with the self-similar transformation. The proposed method is effectively applied to generate new self-similar solutions of the LRT equation. Finally, graphical representations of all the obtained solutions are presented as 3D plots generated using Maple 18.

2020 Mathematics Subject Classifications: 35Qxx, 26A33

Key Words and Phrases: Lin–Reissner–Tsien equation, power index method, self-similar transformation, self-similar solutions, nonlinear partial differential equations

1. Introduction

Many real-world physical phenomena are described by nonlinear partial differential equations (NLPDEs). Consequently, studying these equations to assess their integrability and determine exact solutions is essential. While this task is challenging, several analytical techniques have been developed by researchers to obtain exact solutions. Among these are the Exp-Function Method [1], Modified Exp-Function Method [2], [3], [4], Simple Equations Method (SEsM) [5], [6], [7], [8], Sine-Cosine Method [9], [10], First Integral Method [11], [12], Sardar Sub-Equation Method [13], Modified Sardar Sub-Equation Method [14],

*Corresponding author.
DOI: https://doi.org/10.29020/nybg.ejpam.v18i3.6248

Email addresses: 211904@students.au.edu.pk (Z. Haider), khalilmalik@au.edu.pk (K. Ahmad), marif@psu.edu.sa (M. S. Arif), airshad@psu.edu.sa (A. U. Rehman), 211900@students.au.edu.pk (M. N. Qureshi)

[15], Modified Extended Direct Algebraic Method [16], [17], $(\frac{G'}{G})$-Expansion Method [18], Lie Symmetry Method [19], the Hirota Bilinear Method [20], and the Power Index Method [21], [22].

In this paper, we examine the $(2+1)$-dimensional Lin–Reissner–Tsien (LRT) equation:

$$2u_{xt} + u_x u_{xx} - u_{yy} = 0. \tag{1}$$

which represents a significant class of nonlinear partial differential equations (NPDEs) that plays a crucial role in high-speed aerodynamic applications, particularly in the analysis of transonic flow phenomena around airfoil surfaces. The Lin–Reissner–Tsien (LRT) equation mathematically characterizes the complex transitional flow regime around aerodynamic surfaces, where the term u_{xt} represents unsteady flow effects, $u_x u_{xx}$ captures nonlinear wave steepening, and u_{yy} accounts for spanwise pressure gradients. Physically, u is the potential of the velocity field, x and y are the spatial coordinates, and t represents the temporal coordinate in equation (1).

Several researchers have successfully derived self-similar and exact analytic solutions for the Lin–Reissner–Tsien (LRT) equation. Haussermann, Vajravelu, and Van Gorder [23] derived and analyzed self-similar solutions for the LRT equation, a nonlinear partial differential equation governing high-speed fluid flows. The authors employed symmetry reduction techniques to transform the partial differential equation (PDE) into an ordinary differential equation (ODE), obtaining exact solutions that describe the system's behavior under scaling invariance. Filimonov [24] employed a novel special series method to construct analytic solutions for the LRT equation. This approach systematically generates exact solutions and offers new representations that capture the equation's complex dynamics. Theaker and Van Gorder [25] analyzed both forced and unforced forms of the LRT equation, which govern transonic gas flows at various length scales, deriving exact and asymptotic solutions to characterize the flow dynamics.

While the Lin–Reissner–Tsien (LRT) equation has been extensively studied through traditional analytical and numerical approaches, several critical gaps remain in the literature regarding its self-similar solutions and their systematic derivation via the Power Index Method (PIM). This study introduces self-similar solutions to the LRT equation through the Power Index Method–an innovative approach that has been scarcely explored for this class of nonlinear partial differential equations (NLPDEs). By leveraging the inherent scaling symmetries of the LRT equation, we demonstrate how self-similarity systematically decouples the variables and reduces the governing partial differential equation (PDE) into a more tractable ordinary differential equation (ODE). This transformation not only simplifies the analytic treatment but also reveals critical insights into the equation's long-time behavior and singularity formation, which often remain obscured in traditional symmetry-based or numerical approaches. The Power Index Method further distinguishes itself by rigorously determining scaling exponents, bypassing ad hoc assumptions, and offering a unified framework to address multi-parameter nonlinearities. Our work thus bridges a significant gap in the literature, providing a robust analytical tool to explore scale-invariant phenomena in high-speed aerodynamics and beyond.

While numerous analytical and numerical techniques [26], [27] have been developed to

solve nonlinear partial differential equations, the Power Index Method (PIM) offers a distinctive and systematic approach grounded in the theory of scaling symmetries. Unlike many recognized methods that often rely on predefined ansätze, functional assumptions, or trial solution forms, PIM derives self-similar transformations directly from the intrinsic scaling properties of the governing equation. This avoids arbitrary guesswork and ensures that the resulting similarity variables are mathematically consistent with the equation's structure. Furthermore, PIM rigorously determines the scaling exponents by balancing the dominant terms in the original equation, providing a clear theoretical foundation rooted in dimensional analysis and self-similarity theory. This process transforms the original PDE into an ordinary differential equation (ODE) without requiring symmetry generators or complicated algebraic frameworks. As such, PIM not only broadens the class of solvable equations but also enhances transparency and reproducibility in the solution process, making it a powerful alternative for deriving exact, self-similar solutions to nonlinear PDEs.
The role of similarity transformations in deriving self-similar solutions to the Lin–Reissner–Tsien (LRT) equation is pivotal, as these transformations facilitate the reduction of complex partial differential equations into more manageable ordinary differential equations. This process allows for the identification of exact solutions and enhances understanding of transonic flows. While similarity transformations are powerful tools for deriving self-similar solutions, they may not capture the full dynamics of the system, particularly in cases of rapid wave propagation or complex boundary conditions which could necessitate the alternative analytical or numerical approaches.
The paper is structured as follows: In Section 2, we briefly describe the Power Index Method (PIM). In Section 3, we apply this method to the Lin–Reissner–Tsien (LRT) equation using a self-similar function transformation and derive its self-similar solution. The results and discussion are presented in Section 4, followed by the conclusions in Section 5. Finally, future recommendations are provided in Section 6.

2. Power Index Method

Step:-1
Consider the nonlinear partial differential equation (1), for which we seek an exact solution. To facilitate this, we introduce the wave variable ξ, defined as a combination of the independent variables x, y, and t, each raised to a specific power-law exponent:

$$\xi = x^m y^r t^p. \tag{2}$$

Here, m, r, and p are constants to be determined. In a similar manner, we assume a self-similar transformation for the dependent variable $u(x, y, t)$ expressed in terms of the similarity variable ξ:

$$u = x^n y^s t^q f(\xi). \tag{3}$$

In this expression, n, s, and q are additional exponents to be determined, and $f(\xi)$ represents the unknown function to be solved.
Step:-2

We now differentiate equations (2) and (3) with respect to the original PDE (1) in order to determine the relationships among the exponents of x, y, and t in each term. Substituting these into equation (1), the nonlinear partial differential equation is transformed into a mixed algebraic form as follows:

$$F(t,x,y) = t^{A_t} x^{A_x} y^{A_y} \phi(\xi, g'(\xi), g''(\xi), ...). \tag{4}$$

The resulting relationships among the exponents can be represented by the following functions:

$$A_t = a_1 p + a_2 q + a_3. \tag{5}$$

$$A_x = b_1 m + b_2 n + b_3. \tag{6}$$

$$A_y = c_1 r + c_2 s + c_3. \tag{7}$$

By analyzing the coefficients of A_t, A_x, and A_y, we ensure that the partial differential equation (PDE) given in equation (1) can be reduced to an ordinary differential equation (ODE). The optimal exponents for x, y, and t are selected such that only three indices are allowed to vary simultaneously, while the remaining exponents are treated as fixed constants. We repeat this process with different indices of x, y, and t to find all well-defined transformations.

Step:-3

Upon substituting the power-law exponents into the transformation, the partial differential equation (PDE) given in equation (1) is reduced to an ordinary differential equation (ODE) in terms of the function $f(\xi)$.

$$G(\xi, f(\xi), f'(\xi), f''(\xi), f'''(\xi), ...) = 0. \tag{8}$$

Step:-4

The solution of the ordinary differential equation (ODE) given in eqaution (8) is obtained

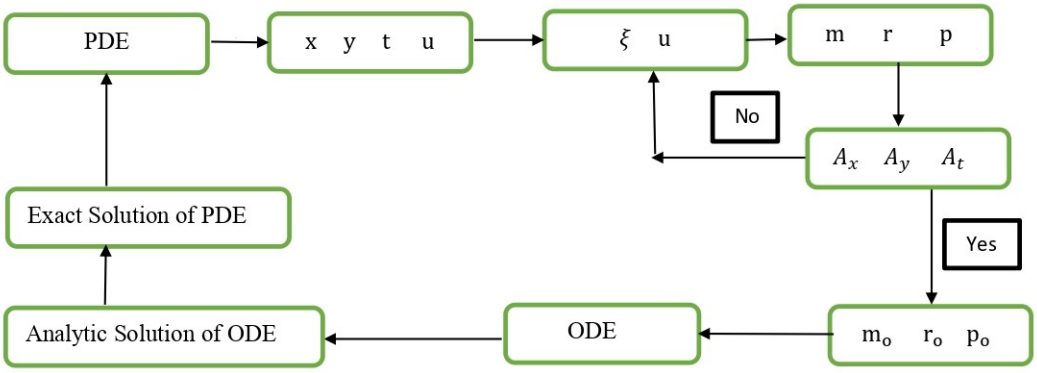

Figure 1: **Flow Chart of Power Index Method**

by using computerized symbolic package like Maple 18 and basic techniques. Subsequently, the exact solution of equation (1) is derived by substituting the obtained function $f(\xi)$ into the transformation defined in equation (3).

3. New Self-Similar Solutions of Lin–Reissner–Tsien Equation

Case:-1

We consider the self-similar function transformation given by:

$$\xi = \frac{x}{t^m}. \tag{9}$$

$$u = t^n f(\xi). \tag{10}$$

where m and n are constants to be determined. Differentiating equations (9) and (10) with respect to equation (1) yields the following partial derivatives:

$$u_{xt} = t^{n-m-1}(nf^{'}(\xi) - m\xi f^{''}(\xi) - mf^{'}(\xi)). \tag{11}$$

$$u_x = t^{n-m} f^{'}(\xi). \tag{12}$$

$$u_{xx} = t^{n-2m} f^{''}(\xi). \tag{13}$$

$$u_{yy} = 0. \tag{14}$$

Substituting equations (11), (12), (13), and (14) into equation (1) yields:

$$2(n-m)t^{n-m-1} f^{'}(\xi) - 2mxt^{n-2m-1} f^{''}(\xi) + t^{2n-3m} f^{'}(\xi) f^{''}(\xi) = 0. \tag{15}$$

Since $\xi = \frac{x}{t^m}$, equation (15) simplifies to:

$$2(n-m)t^{n-m-1} f^{'}(\xi) - 2mt^{n-m-1}\xi f^{''}(\xi) + t^{2n-3m} f^{'}(\xi) f^{''}(\xi) = 0. \tag{16}$$

Dividing both sides of equation (16) by t^{n-m-1}, we obtain:

$$2(n-m)f^{'}(\xi) - 2m\xi f^{''}(\xi) + t^{n-2m+1} f^{'}(\xi) f^{''}(\xi) = 0. \tag{17}$$

The last term in equation (17) involves the factor t^{n-2m+1}, which must reduce to unity (i.e., t^0) to preserve dimensional consistency. This requirement yields the scaling relation $n = 2m - 1$. For selected values of m and n, we are able to find the solutions of ODE (17). However, for arbitrary values of these parameters, the general solution of the ODE (17) cannot be obtained.

$n = 2m-1$	m	-1	1
	n	-3	1

Table 1. Specific values of m and n for obtainig exact solutions

Family Solutions

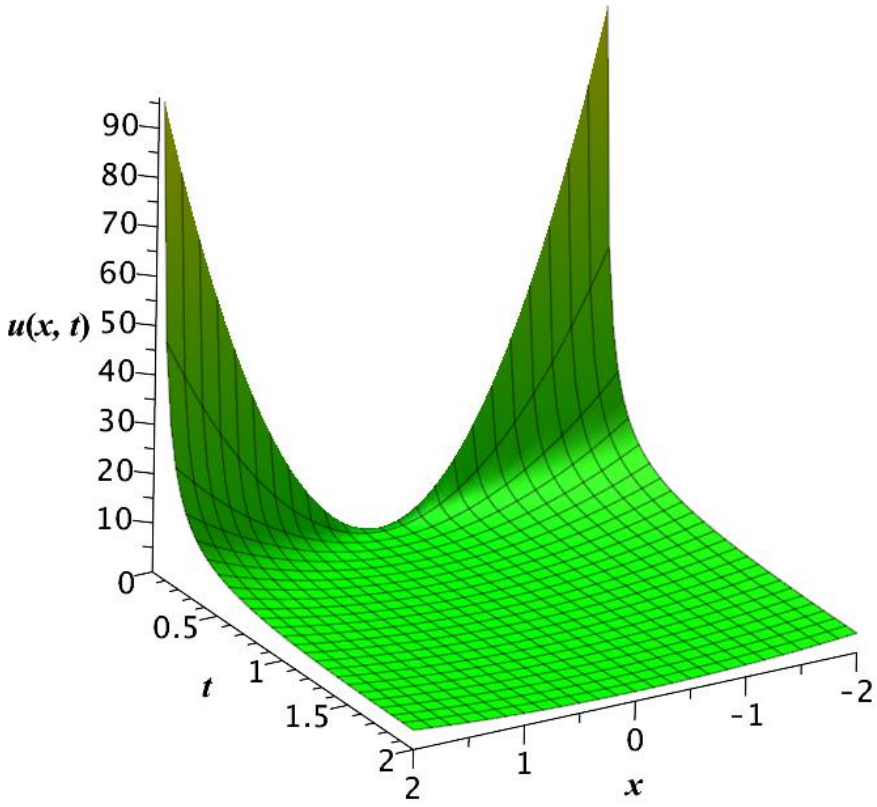

Figure 2: 3D plot of (24) for $C = 1$.

(i) For the parameter values $m = 1$ and $n = 1$, the similarity function transformation given in equations (9) and (10) reduce to the form:

$$\xi = \frac{x}{t}. \tag{18}$$

$$u = tf(\xi). \tag{19}$$

Substituting the parameter values $m = 1$ and $n = 1$ in equation (17), we obtain the following ordinary differential equation (ODE):

$$-2\xi f''(\xi) + f'(\xi)f''(\xi) = 0. \tag{20}$$

We rewrite equation (20) in factored form:

$$f''(\xi)(f'(\xi) - 2\xi) = 0. \tag{21}$$

This factored form suggests two possibilities, since the product of two terms is zero:

i. $f''(\xi) = 0$ (Trivial Case)

ii. $f'(\xi) - 2\xi = 0$ (Non-trivial Case)

We focus on the non-trivial case:

$$f'(\xi) - 2\xi = 0.$$

$$f'(\xi) = 2\xi. \tag{22}$$

Integrate both sides of equation (22) w.r.t ξ, we obtain:

$$f(\xi) = \xi^2 + C. \tag{23}$$

where C is an arbitrary constant of integration. Applying the similarity transformations (18) and (19), together with the analytic solution of ODE in equation (23), we derive the exact solution to the original PDE (1):

$$u(x,t) = \frac{x^2 + Ct^2}{t}. \tag{24}$$

(ii) For the parameter values $m = -1$ and $n = -3$, the similarity transformations given in equations (9) and (10) reduce to:

$$\xi = xt. \tag{25}$$

$$u = \frac{f(\xi)}{t^3}. \tag{26}$$

Substituting the parameter values $m = -1$ and $n = -3$ into equation (17), we obtain the following ordinary differential equation (ODE):

$$2\xi f''(\xi) + f'(\xi)f''(\xi) - 4f'(\xi) = 0. \tag{27}$$

To simplify, we let $u = f'(\xi)$ and $u' = f''(\xi)$. Then equation (27) becomes:

$$2\xi u' + uu' - 4u = 0. \tag{28}$$

Rewriting equation (28) in a solvable form, we obtain:

$$u' = \frac{4u}{u + 2\xi}. \tag{29}$$

Assuming $u = v\xi$, so that $u' = v + v'\xi$, and substituting into equation (29), we obtain:

$$(\frac{1}{v} + \frac{2}{2 - v})dv = \frac{1}{\xi}d\xi. \tag{30}$$

Integrating both sides of equation (30) yields:

$$\ln v - 2\ln(2 - v) = \ln \xi + \ln C_1. \tag{31}$$

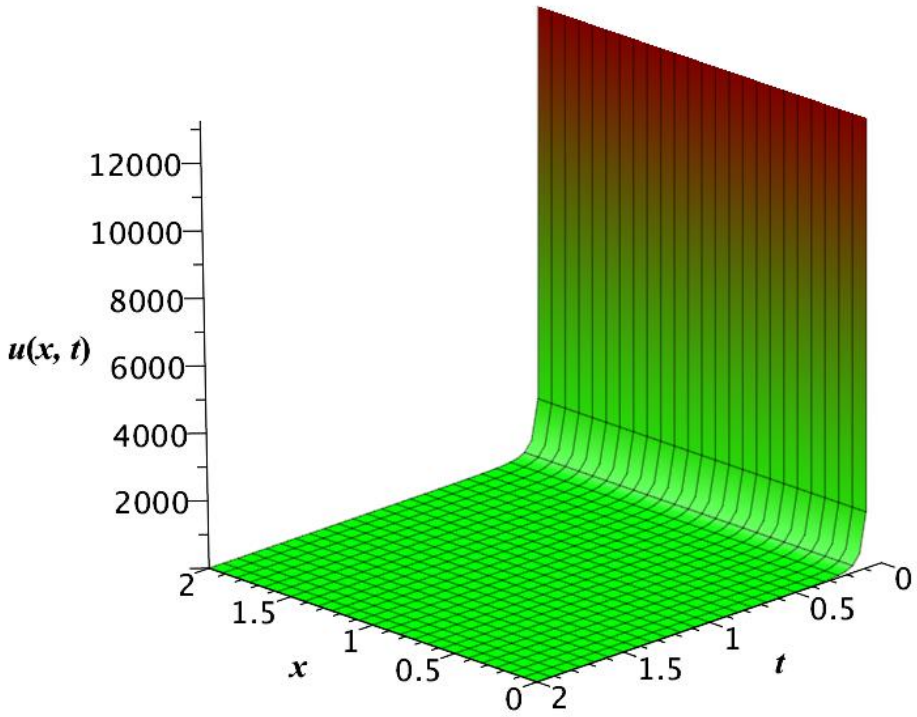

Figure 3: 3D plot of (36) for $C_1 = 1$ and $C_2 = 1$.

Simplifying equation (31), we obtain:

$$v\xi = \frac{(4C_1\xi + 1) + \sqrt{8C_1\xi + 1}}{2C_1}. \tag{32}$$

Since $v\xi = u$ and $u = f'(\xi)$, equation (32) becomes:

$$f'(\xi) = \frac{(4C_1\xi + 1) + \sqrt{8C_1\xi + 1}}{2C_1}. \tag{33}$$

After simplification, equation (33) becomes:

$$f'(\xi) = 2\xi + \frac{1}{2C_1} + \frac{\sqrt{8C_1\xi + 1}}{2C_1}. \tag{34}$$

Integrating both sides of equation (34) gives the analytic solution to the ODE (27):

$$f(\xi) = \xi^2 + \frac{\xi}{2C_1} + \frac{(8C_1\xi + 1)^{\frac{3}{2}}}{24C_1^2} + C_2. \tag{35}$$

Using the similarity transformations (25) and (26), along with the analytic solution of the ODE in equation (35), we obtain the exact solution to the original PDE (1):

$$u(x,t) = \frac{x^2t^2 + \frac{xt}{2C_1} - \frac{(8C_1xt+1)^{\frac{3}{2}}}{24C_1^2} + C_2}{t^3}. \tag{36}$$

Case:-2

We introduce the following similarity function transformation:

$$\xi = \frac{y}{x^m}. \tag{37}$$

$$u = x^n f(\xi). \tag{38}$$

Differentiating equations (37) and (38) with respect to equation (1), we obtain:

$$u_x = nx^{n-1}f(\xi) - myx^{n-m-1}f'(\xi). \tag{39}$$

$$u_{yy} = x^{n-2m}f''(\xi). \tag{40}$$

$$u_{xx} = x^{n-2}(n^2-n)f(\xi) - (2mn\xi + m^2\xi + m\xi)f'(\xi) + m^2y^2x^{-2}f''(\xi). \tag{41}$$

$$u_{xt} = 0. \tag{42}$$

Using equations (39), (40), (41) and (42) in equation (1), we obtain the following ordinary differential equation (ODE):

$$\begin{aligned}&(m^3-n^2)f^2(\xi) + (2mn - 3mn^2 + nm^2)\xi f(\xi)f'(\xi) + n^2m^2\xi^2 f(\xi)f''(\xi)\\ &+ (2m^2n - m^2 - m^3)\xi^2 f'^2(\xi) - m^3\xi^3 f'(\xi)f''(\xi) - x^{-2m-n+3}f''(\xi) = 0.\end{aligned} \tag{43}$$

The last term in equation (43) contains the factor $x^{-2m-n+3}$, which must equal unity (i.e., x^0) to ensure dimensional consistency. This leads to the condition $n = -2m + 3$. For a few values of m and n, we are able to find the solution of ODE (43). However, for all values of these parameters, the general solution of the ODE (43) cannot be obtained.

$n = -2m + 3$	m	1	0
	n	1	3

Table 2. Specific values of m and n for obtainig exact solutions

Family Solutions

(i) For the parameter values $m = 1$ and $n = 1$, the similarity transformations (37) and (38) reduce to:

$$\xi = \frac{y}{x}. \tag{44}$$

$$u = xf(\xi). \tag{45}$$

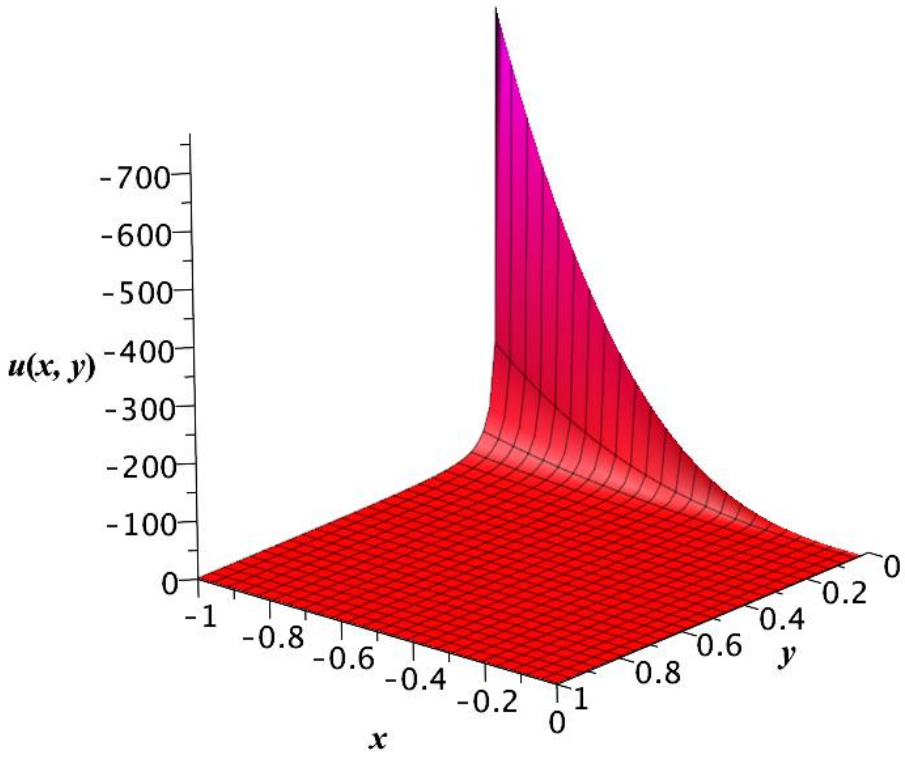

Figure 4: 3D plot of (48) for $C_1 = -2$.

Substituting these values of m and n into equation (43), we obtain the following ODE:

$$\xi^2 f(\xi) f''(\xi) - \xi^3 f'(\xi) f''(\xi) - f''(\xi) = 0. \tag{46}$$

The analytic solution to ODE (46) is:

$$f(\xi) = \frac{1}{3\xi^2} + C_1 \xi. \tag{47}$$

Using the similarity function transformations (44), (45) and the analytic solution of ODE (47), we derive the exact solution to PDE (1):

$$u(x, y) = \frac{x^3 + 3C_1 y^3}{3y^2}. \tag{48}$$

(ii) For $m = 0$ and $n = 3$, the similarity transformations (37) and (38) reduce to:

$$\xi = y. \tag{49}$$

$$u = x^3 f(\xi). \tag{50}$$

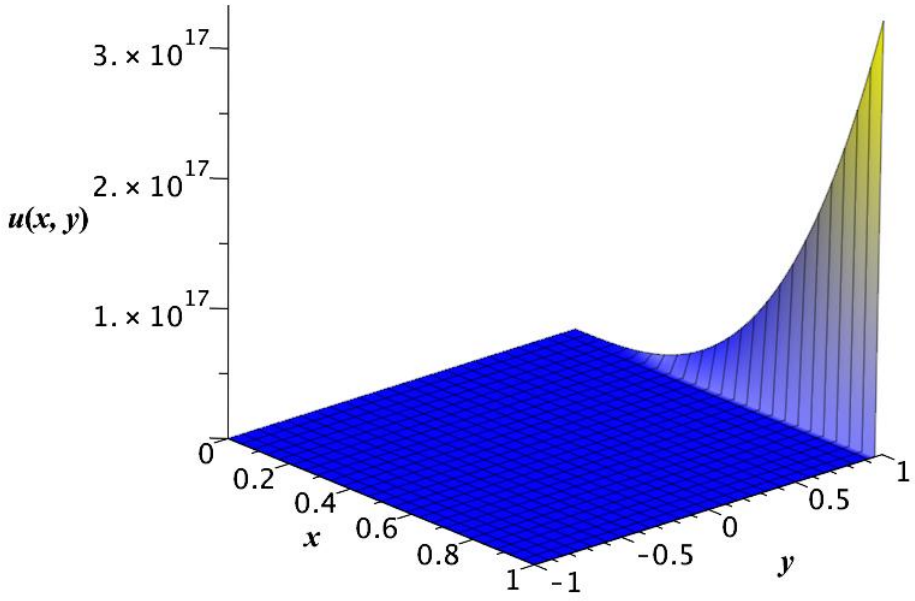

Figure 5: 3D plot of (53) for $C_1 = -1$ and $C_2 = 1$.

Substituting these parameter values into equation (43), we obtain the following ODE:

$$18f^2(\xi) - f''(\xi) = 0. \tag{51}$$

The analytic solution to ODE (51) is expressed in terms of the Weierstrass elliptic function:

$$f(\xi) = \frac{1}{3}\wp(\xi + C_1; g_2, g_3). \tag{52}$$

The Weierstrass elliptic function is defined as:

$$\wp(\xi; g_2, g_3) = \frac{1}{\xi^2} + \sum_{\omega \in \Lambda \setminus \{0\}} \left(\frac{1}{(\xi - \omega)^2} - \frac{1}{\omega^2} \right).$$

The corresponding exact solution of PDE (1) is:

$$u(x, y) = \frac{x^3}{3}\wp(y + C_1; 0, C_2). \tag{53}$$

In equation (53), $\wp$ denotes the Weierstrass elliptic function, which plays a fundamental role in solving certain nonlinear differential equations. Here, $g_2 = 0$ and $g_3 = C_2$.

Remark:-
The Weierstrass elliptic function $\wp(z; g_2, g_3)$ is a doubly periodic meromorphic function with branch points occuring where the discriminant $\Delta = g_2^3 - 27g_3^2$ vanishes. Its branch structure and complex periodicity must be carefully analyzed, as they affect the solution's analyticity and physical interpretation—particularly in modeling nonlinear wave structures and oscillatory flow fields. In aerodynamics, Weierstrass functions are valuable for describing periodic or solitary wave patterns in nonlinear potential flows and boundary layer separation phenomena.

Case:-3
We choose the similarity function transformation as

$$\xi = xe^{at}. \tag{54}$$

$$u = e^{-bt} f(\xi). \tag{55}$$

Differentiating equations (54) and (55) according to equation (1), we get

$$u_x = e^{t(a-b)} f'(\xi). \tag{56}$$

$$u_{xx} = e^{t(2a-b)} f''(\xi). \tag{57}$$

$$u_{xt} = -bf'(\xi) + a\xi f''(\xi) + af'(\xi). \tag{58}$$

$$u_{yy} = 0. \tag{59}$$

Substituting equations (56), (57), (58) and (59) into equation (1), we obtain an ordinary differential equation (ODE) of the following form:

$$-2bf'(\xi) + 2axe^{at} f''(\xi) + 2af'(\xi) + e^{t(2a-b)} f'(\xi) f''(\xi) = 0. \tag{60}$$

Since $\xi = xe^{at}$, equation (60) becomes:

$$-2bf'(\xi) + 2a\xi f''(\xi) + 2af'(\xi) + e^{t(2a-b)} f'(\xi) f''(\xi) = 0. \tag{61}$$

The last term in equation (61) contains the factor $e^{t(2a-b)}$, which must equal unity (i.e., e^0). This requirement yields the relation $b = 2a$. Although it is possible to find solutions to the ODE (61) for general values of a and b, we consider specific values of these parameters to obtain exact solutions.

$b = 2a$	a	$\frac{1}{2}$	-1
	b	1	-2

Table 3. Specific values of a and b for obtainig exact solution

Family Solutions

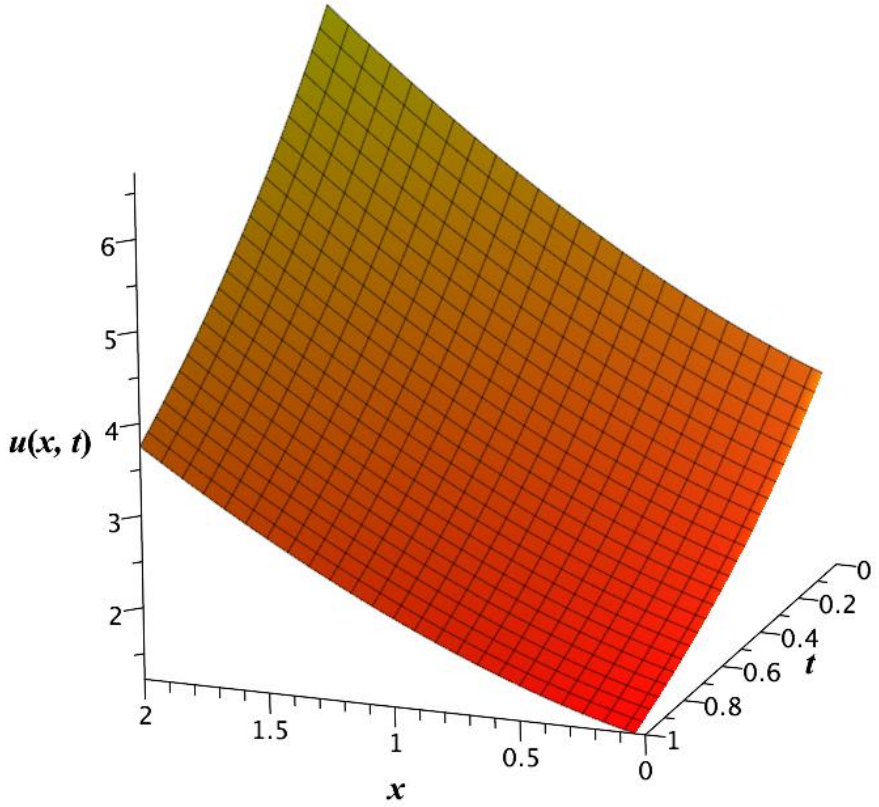

Figure 6: 3D plot of (66) for $C_1 = 1$ and $C_2 = 3$.

(i) For the parameter values $a = \frac{1}{2}$ and $b = 1$, the similarity transformation given in equations (54) and (55) become:

$$\xi = xe^{\frac{t}{2}}. \tag{62}$$

$$u = e^{-t} f(\xi). \tag{63}$$

Using these parameter values in equation (61), we obtain the the following ordinary differential equation (ODE):

$$-f'(\xi) + \xi f''(\xi)) + f'(\xi) f''(\xi) = 0. \tag{64}$$

The analytic solution to ODE (64) is:

$$f(\xi) = \frac{(2\text{LambertW}(C_1\xi) + 1)\xi^2}{4\text{LambertW}(C_1\xi)^2} + C_2. \tag{65}$$

Using the similarity function transformations (62) and (63), together with the analytic solution of the ODE (65), we obtain the exact solution of the PDE (1):

$$u(x,t) = \frac{e^{-t}(2\text{LambertW}(C_1 x e^{\frac{t}{2}}) + 1)x^2 e^t}{4\text{LambertW}(C_1 x e^{\frac{t}{2}})^2} + C_2. \tag{66}$$

(ii) For the parameter values $a = -1$ and $b = -2$, the similarity function transformations (54) and (55) become:

$$\xi = x e^{-t}. \tag{67}$$

$$u = e^{-2t} f(\xi). \tag{68}$$

Using these parameter values in equation (61), we obtain the following ordinary differential equation (ODE):

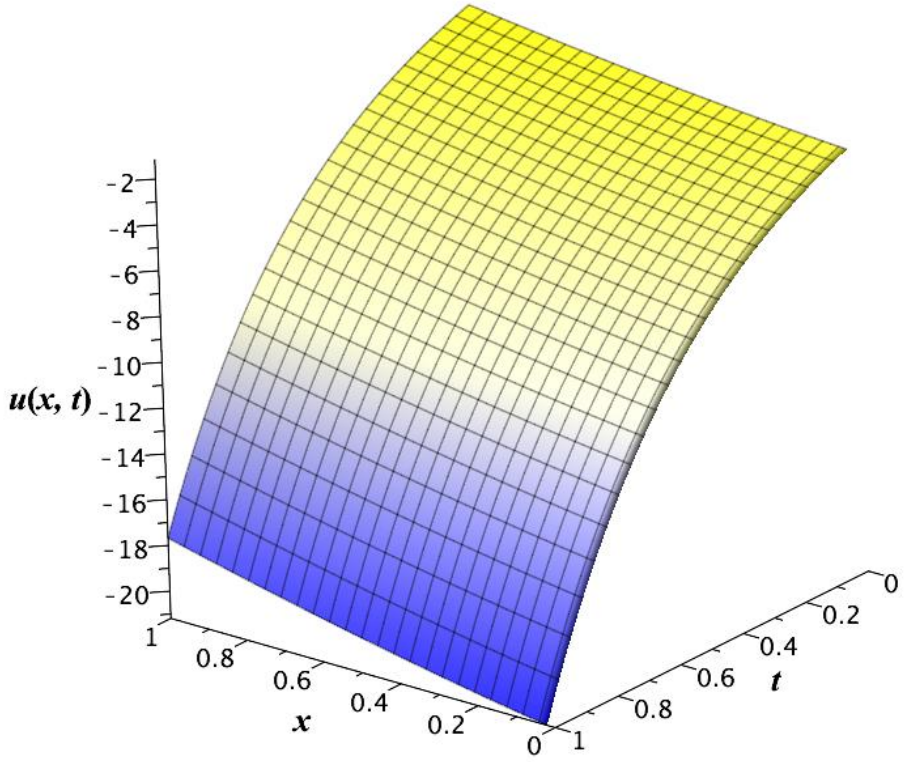

Figure 7: 3D plot of (71) for $C_1 = -1$ and $C_2 = -3$.

$$2f'(\xi) - 2\xi f''(\xi)) + f'(\xi)f''(\xi) = 0. \tag{69}$$

The exact solution to ODE (69) is:

$$f(\xi) = \frac{(2\text{LambertW}(-2C_1\xi) + 1)\xi^2}{2\text{LambertW}(-2C_1\xi)^2} + C_2. \tag{70}$$

Using the similarity function transformations (67) and (68), together with the analytic solution of the ODE (70), we obtain the exact solution of the PDE (1):

$$u(x,t) = \frac{(2\text{LambertW}(-2C_1xe^{-t}) + 1)x^2}{2\text{LambertW}(-2C_1xe^{-t})^2} + C_2e^{2t}. \tag{71}$$

Remark:-
The LambertW function, defined as the inverse of $We^W = Z$, is multivalued with two real branches: the principal branch W_0, defined for $Z \geq -\frac{1}{e}$, and the lower branch W_{-1} defined for $\frac{1}{e} \leq z \leq 0$. The branch point at $z = -\frac{1}{e}$ and corresponding branch cuts play a critical role in ensuring the physical validity and continuity of solutions in aerodynamic models, especially when dealing with exponential growth or decay in boundary layers or transonic flows. In aerodynamics, LambertW function appears in exact solutions of nonlinear equations involving compressible flow and similarity reductions.

Case:-4
We introduce the elementary exponential function transformation, defined as:

$$\xi = e^{mx+ny}. \tag{72}$$

$$u = f(\xi). \tag{73}$$

Differentiating equations (72) and (73) according to equation (1), we obtain:

$$u_x = m\xi f'(\xi). \tag{74}$$

$$u_{xx} = m^2\xi(\xi f''(\xi) + f'(\xi)). \tag{75}$$

$$u_{yy} = n^2\xi(\xi f''(\xi) + f'(\xi)). \tag{76}$$

$$u_{xt} = 0. \tag{77}$$

Substiuting equations (74), (75), (76), and (77) in equation (1), we obtain the following ODE:

$$m^3\xi^2 f'(\xi)f''(\xi) + m^3\xi f'^2(\xi) - n^2\xi f''(\xi) - n^2 f'(\xi) = 0. \tag{78}$$

The analytic solution to ODE (78) is:

$$f(\xi) = \frac{n^2\ln(\xi) + \ln(\xi)\sqrt{-2C_1m^3 + n^4}}{m^3} + C_2. \tag{79}$$

Using the similarity function transformations (72) and (73), together with the analytic solution of ODE (79), we obtain the exact solution to the PDE (1):

$$u(x,y) = \frac{n^2(mx+ny) + (mx+ny)\sqrt{-2C_1m^3 + n^4}}{m^3} + C_2. \tag{80}$$

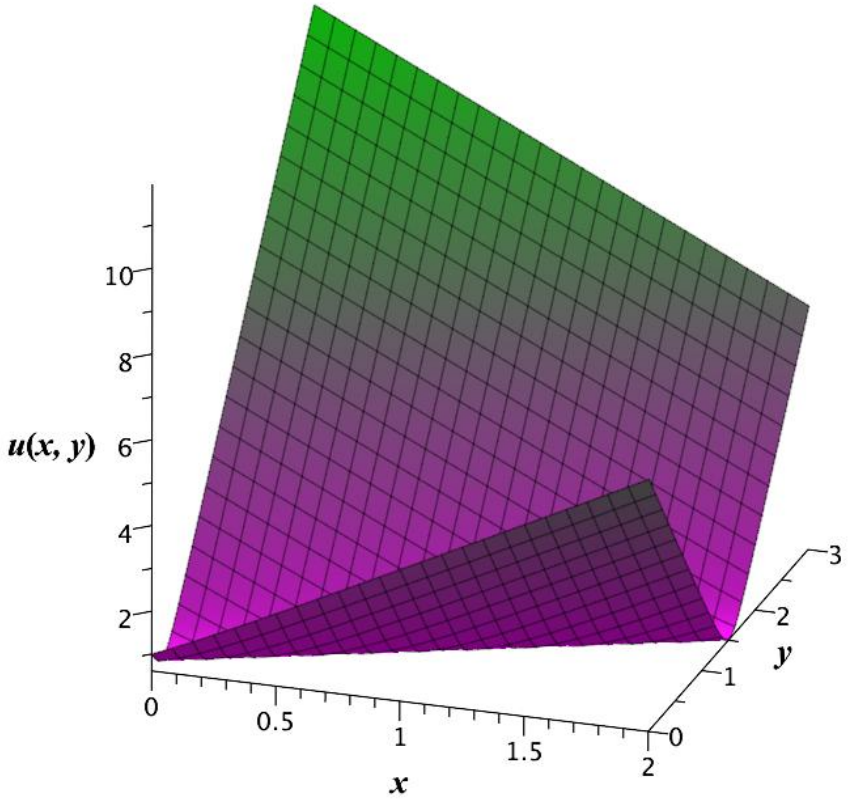

Figure 8: 3D complex plot of (80) for $m = -2$, $n = 3$, $C_1 = -8$ and $C_2 = 1$.

Convergence of Self-Similar Solutions

The self-similar solutions derived in this study are constructed through exact analytical transformations that reduce the original partial differential equations to simpler forms. The convergence of these solutions is ensured by identifying and excluding singular points from the solution domain, such as values that lead to division by zero or non-real expressions (e.g., due to square roots or special functions). Under appropriate conditions on the parameters and variables, the solutions remain real-valued, continuous, and physically meaningful, confirming their validity and convergence within the defined domains.

4. Results and Discussion

This work introduces a novel analytical framework for obtaining self-similar solutions of the Lin–Reissner–Tsien (LRT) equation, offering new insights into nonlinear dynamical systems. The Power Index Method (PIM) yields self-similar solutions with distinct structures, including traveling waves, blow-up singularities, boundary layers, dissipative

solitons, and localized pulses–each emerging from the scaling symmetries and nonlinear nature of the governing partial differential equation.
Fig. 2 depicts a spatial blow-up solution exhibiting time-decaying behavior, the solution $u(x,t)$ becomes unbounded as $|x| \to \infty$, indicating spatial blow-up, while simultaneously decaying in time as t increases. This dual behavior is typical of certain nonlinear PDEs where localized structures dissipate over time but exhibit singularities or steep spatial gradients. Fig. 3 represents a shock wave or boundary layer solution, characterized by steep spatial gradients indicative of singular perturbation effects. Such solutions correspond to abrupt transitions in fluid properties like velocity, pressure, and density–phenomena commonly observed in supersonic or transonic flows. Fig. 4 illustrates a finite-time blow-up solution, showing an explosive growth in amplitude. Blow-up phenomena, where solutions become unbounded in finite time or space, are significant in modeling wave breaking, turbulence onset, and flow singularities near critical points in compressible flow systems. Fig. 5 presents a damped oscillatory solution, characterized by its decaying amplitude and wave-like temporal behavior. Fig. 6 displays a localized stationary soliton solution, which maintains a stable, peaked profile without dispersing over time. Soliton solutions are smooth, localized waveforms that retain their shape due to a balance between nonlinearity and dispersion. They are particularly important in modeling non-dispersive wave interactions in nonlinear media, including boundary layer effects and internal fluid waves. These mathematical structures provide insight into the qualitative behavior of solutions and help interpret complex nonlinear flow features relevant to engineering and physical applications such as aerodynamic systems, gas dynamic processes, and transonic regimes. Fig. 7 illustrates a self-similar solution of the second kind, characterized by a dynamically evolving profile that preserves its shape under scaling transformations while exhibiting power-law temporal decay. Fig. 8 shows a nonlinear standing wave solution with a periodic spatial structure and amplitude modulated by the interplay between nonlinearity and dispersion.
This paper serves as a valuable resource for scientists and researchers by offering thorough analysis and clear graphical representations that enhance the understanding of the LRT equation's dynamic behavior and associated physical phenomena. Furthermore, it opens new research directions across multiple scientific disciplines by demonstrating the effectiveness of the Power Index Method in solving nonlinear partial differential equations.

5. Conclusions

This research paper aims to derive self-similar solutions involving rational, exponential, and special functions, obtained from the Lin–Reissner–Tsien (LRT) equation through the application of the Power Index Method (PIM). The solutions are presented in explicit form and depend on the independent variables. Through self-similar transformations of the nonlinear LRT equation, we derive nonlinear ordinary differential equations (ODEs) with parameter-dependent coefficients. Using the symbolic computation software Maple 18, we obtain analytic solutions to the resulting nonlinear ODEs. The self-similar solutions of the Lin–Reissner–Tsien equation are obtained using these transformations and the analytic

solutions of the corresponding ODEs. All obtained solutions are novel, with some expressed in terms of special functions ((refer to ((53), (66) and (71)). The exact solutions of the LRT equation presented in this study provide valuable insights into various physical phenomena. Additionally, the projective Power Index Method has been effectively utilized to obtain these exact solutions.

6. Future Recommendations

The study of self-similar solutions to the Lin–Reissner–Tsien (LRT) equation using the Power Index Method (PIM) offers multiple avenues for further investigation. First, extending the method to higher-dimensional or more complex flow configurations could enhance its applicability in aerodynamics and fluid dynamics. Investigating the stability and physical realizability of obtained solutions through numerical simulations or experiments would provide deeper insights into their practical relevance. Additionally, incorporating variable power indices or nonlinear transformations might uncover new classes of self-similar solutions. Exploring connections with other asymptotic methods, such as Lie symmetry analysis or perturbation techniques, could further unify the theoretical framework. Finally, applying these solutions to real-world problems, such as hypersonic flows or boundary layer phenomena, would validate their utility and potentially lead to novel engineering applications.

Acknowledgements

The authors wish to express their gratitude to Prince Sultan University for facilitating the publication of this article through the Theoretical and Applied Sciences Lab.

Funding Statement

The authors would like to acknowledge the support of Prince Sultan University for paying the Article Processing Charges (APC) of this publication.

Competing interests

The authors declare that they have no competing interests.

Data Availability Statement

The computations and results presented in this study are based entirely on symbolic analysis performed using Maple 18 software. While no empirical datasets were generated or analyzed, the corresponding Maple 18 worksheets that contain all derivations and solution steps are available from the authors upon reasonable request to ensure full transparency and reproducibility of the work.

References

[1] Sajid, N.; Perveen, Z.; Sadaf, M.; Akram, G.; Abbas, M.; Abdeljawad, T.; Alqudah, M.A. *Implementation of the Exp-function approach for the solution of KdV equation with dual power law nonlinearity*. Comput. Appl. Math. **2022**, *41*, 338.

[2] Attaullah; Shakeel, M.; Shah, N.A.; Chung, J.D. *Modified exp-function method to find exact solutions of ionic currents along microtubules*. Mathematics **2022**, *10*, 851.

[3] Shakeel, M.; Shah, N.A.; Chung, J.D. *Application of modified exp-function method for strain wave equation for finding analytical solutions*. Ain Shams Eng. J. **2023**, *14*, 101883.

[4] Shakeel, M.; Attaullah; Shah, N.A.; Chung, J.D. *Modified exp-function method to find exact solutions of microtubules nonlinear dynamics models*. Symmetry **2023**, *15*, 360.

[5] Vitanov, N.K.; Dimitrova, Z.I. *Simple Equations Method and non-linear differential equations with non-polynomial non-linearity*. Entropy **2021**, *23*, 1624.

[6] Vitanov, N.K.; Dimitrova, Z.I.; Vitanov, K.N. *On the use of composite functions in the Simple Equations Method to obtain exact solutions of nonlinear differential equations*. Computation **2021**, *9*, 104.

[7] Vitanov, N.K. *Simple Equations Method (SEsM): An effective algorithm for obtaining exact solutions of nonlinear differential equations*. Entropy **2022**, *24*, 1653.

[8] Tajadodi, H.; Khan, Z.A.; Gómez-Aguilar, J.F.; Khan, A.; Khan, H. *Exact solutions of conformable fractional differential equations*. Results Phys. **2021**, *22*, 103916.

[9] Ala, V.; Shaikhova, G. *Analytical solutions of nonlinear beta fractional Schrödinger equation via sine-cosine method*. Lobachevskii J. Math. **2022**, *43*, 3033–3038.

[10] Behera, S. *Multiple soliton solutions of some conformable fractional nonlinear models using Sine–Cosine method*. Opt. Quantum Electron. **2024**, *56*, 1235.

[11] Behera, S. *Analysis of traveling wave solutions of two space-time nonlinear fractional differential equations by the first-integral method*. Mod. Phys. Lett. B **2024**, *38*, 2350247.

[12] Ghosh, A.; Maitra, S. *The first integral method and some nonlinear models*. Comput. Appl. Math. **2021**, *40*, 79.

[13] Yasin, S.; Khan, A.; Ahmad, S.; Osman, M.S. *New exact solutions of (3+1)-dimensional modified KdV-Zakharov-Kuznetsov equation by Sardar-subequation method*. Opt. Quantum Electron. **2024**, *56*, 90.

[14] Ahmad, J.; Hameed, M.; Mustafa, Z.; Rehman, S.U. *Soliton patterns in the truncated M-fractional resonant nonlinear Schrödinger equation via modified Sardar subequation method*. J. Opt. **2024**, 1–22.

[15] Kamel, N.M.; Ahmed, H.M.; Rabie, W.B. *Retrieval of soliton solutions for 4th-order (2+1)-dimensional Schrödinger equation with higher-order odd and even terms by modified Sardar sub-equation method*. Ain Shams Eng. J. **2024**, *15*, 102808.

[16] Ghayad, M.S.; Badra, N.M.; Ahmed, H.M.; Rabie, W.B. *Derivation of optical solitons and other solutions for nonlinear Schrödinger equation using modified extended direct algebraic method*. Alexandria Eng. J. **2023**, *64*, 801–811.

[17] Bilal, M.; Iqbal, J.; Shah, K.; Abdalla, B.; Abdeljawad, T.; Ullah, I. *Analytical solu-*

tions of the space–time fractional Kundu–Eckhaus equation by using modified extended direct algebraic method. Partial Differ. Equ. Appl. Math. **2024**, *11*, 100832.

[18] Mohanty, S.K.; Kumar, S.; Dev, A.N.; Deka, M.K.; Churikov, D.V.; Kravchenko, O.V. *An efficient technique of* $(\frac{G'}{G})$*–expansion method for modified KdV and Burgers equations with variable coefficients*. Results Phys. **2022**, *37*, 105504.

[19] Jhangeer, A.; Ansari, A.R.; Imran, M.; Riaz, M.B. *Lie symmetry analysis, and traveling wave patterns arising the model of transmission lines*. AIMS Math. **2024**, *9*, 18013–18033.

[20] Yang, L.; Gao, B. *Multiple solitons solutions, lump solutions and rogue wave solutions of the complex cubic Ginzburg–Landau equation with the Hirota bilinear method*. Indian J. Phys. **2025**, *99*, 221–228.

[21] Haider, Z.; Ahmad, K. *Novel exact solutions for a biological population model using the power index method*. Eur. J. Pure Appl. Math. **2025**, *18*, 5936–5936.

[22] Ahmad, K.; Bibi, K. *New function solutions of Ablowitz-Kaup-Newell-Segur water wave equation via power index method*. J. Funct. Spaces **2022**, *2022*, 9405644.

[23] Haussermann, J.; Vajravelu, K.; Van Gorder, R.A. *Self-similar solutions to Lin–Reissner–Tsien equation*. Appl. Math. Mech. **2011**, *32*, 1447–1456.

[24] Filimonov, M.Y. *Application of the method of special series to the representation of solutions of the Lin–Reissner–Tsien equation*. Proc. Steklov Inst. Math. **2008**, *261*, S55–S76.

[25] Theaker, K.A.; Van Gorder, R.A. *Solutions to forced and unforced Lin–Reissner–Tsien equations for transonic gas flows on various length scales*. Commun. Theor. Phys. **2017**, *67*, 309.

[26] Ahmad, I.; Amin, R.; Abdeljawad, T.; Shah, K. *A numerical method for fractional pantograph delay integro-differential equations on Haar wavelet*. Int. J. Appl. Comput. Math. **2021**, *7*, 1–13.

[27] Rehman, M.U.; Baleanu, D.; Alzabut, J.; Ismail, M.; Saeed, U. *Green–Haar wavelets method for generalized fractional differential equations*. Adv. Difference Equ. **2020**, *2020*, 1–25.